RESEARCH PAPER

RNA Biology 11:1, 76–91; January 2014; © 2014 Landes Bioscience

Combinatorial regulation of lipoprotein lipase by microRNAs during mouse adipogenesis

Maria Bouvy-Liivrand[1,2], Merja Heinäniemi[1,3], Elisabeth John[1], Jochen G Schneider[2,4], Thomas Sauter[1,†], and Lasse Sinkkonen[1,†,*]

[1]Life Sciences Research Unit; University of Luxembourg; Luxembourg, Luxembourg; [2]Luxembourg Centre for Systems Biomedicine; University of Luxembourg; Esch-Sur-Alzette, Luxembourg; [3]Institute of Biomedicine; School of Medicine; University of Eastern Finland; Kuopio, Finland; [4]Saarland University Medical Center; Department of Medicine II; Homburg, Saar, Germany; [†]These authors contributed equally to this work.

Keywords: microRNA, mathematical modelling, combinatorial gene regulation, lipoprotein lipase, adipocyte differentiation

Abbreviations: ActD, Actinomycin D; CEBP, CCAAT/enhancer binding protein; ChIP, chromatin immunoprecipitation; DMSO, dimethylsulfoxide; GR, glucocorticoid receptor; H3K27ac, H3 lysine 27 acetylation; H3K4me3, histone H3 lysine 4 trimethylation; kb, kilobase; LPL, lipoprotein lipase; miRNA, microRNA; nt, nucleotide; PPAR, peroxisome proliferator-activated receptor; qPCR, real-time quantitative PCR; RISC, RNA-induced silencing complex; Rosi, rosiglitazone; RT, reverse transcription; SEM, standard error of mean; TF, transcription factor; UTR, untranslated region

MicroRNAs (miRNAs) regulate gene expression directly through base pairing to their targets or indirectly through participating in multi-scale regulatory networks. Often miRNAs take part in feed-forward motifs where a miRNA and a transcription factor act on shared targets to achieve accurate regulation of processes such as cell differentiation. Here we show that the expression levels of miR-27a and miR-29a inversely correlate with the mRNA levels of lipoprotein lipase (*Lpl*), their predicted combinatorial target, and its key transcriptional regulator peroxisome proliferator-activated receptor gamma (*Pparg*) during 3T3-L1 adipocyte differentiation. More importantly, we show that *Lpl*, a key lipogenic enzyme, can be negatively regulated by the two miRNA families in a combinatorial fashion on the mRNA and functional level in maturing adipocytes. This regulation is mediated through the *Lpl* 3′UTR as confirmed by reporter gene assays. In addition, a small mathematical model captures the dynamics of this feed-forward motif and predicts the changes in *Lpl* mRNA levels upon network perturbations. The obtained results might offer an explanation to the dysregulation of LPL in diabetic conditions and could be extended to quantitative modeling of regulation of other metabolic genes under similar regulatory network motifs.

Introduction

Complex interplay between genetic and environmental factors defines the functional phenotype of living organisms. Integration of these internal and external cues at a single gene level is achieved through combinatorial regulation of gene expression at both transcriptional and post-transcriptional levels. It has been well established that most genes are targeted by multiple transcription factors acting through a number of separate enhancer sites or in an interdependent manner from shared enhancers.[1] Moreover, the stability of the produced mRNAs and their translation can be affected at the post-transcriptional level by multiple factors such as regulatory RNA-binding proteins (RBPs), often expressed in a cell type-specific manner.[2] As our understanding of the complexity of the multiple layers of gene regulation is rapidly advancing, it is becoming increasingly important to estimate the contributions of individual regulators on the final output simultaneously and predict the outcomes of this combinatorial regulation. Development of quantitative systems biology models helps to integrate the multiple levels of gene regulation.[3]

Eukaryotic miRNAs, a considerably large class of non-coding regulatory RNA molecules, have become recognized as crucial factors directing gene expression and development.[4] These transcripts derive from endogenous inter- or intragenic miRNA genes and are generally transcribed by canonical transcription machinery.[5] miRNAs have large cohorts of potential targets with as much as 60% of the transcriptome predicted to be targeted.[6] Importantly, most unique miRNA families can share mRNA targets and a shorter distance of binding between miRNAs has been shown to play a positive role in advancing the repressive effect of multiple miRNAs on one target.[7-9] Different approaches have suggested that miRNAs efficiently render robustness into the patterns of protein expression through participation in various network motifs together with TFs and their common target genes.[10-12] This type of control is extremely important during cellular differentiation and commitment—in order to rapidly react to discrete but abundant signals that drive differentiation,

*Correspondence to: Lasse Sinkkonen; Email: lasse.sinkkonen@uni.lu
Submitted: 03/25/2013; Revised: 12/20/2013; Accepted: 12/23/2013
http://dx.doi.org/10.4161/rna.27655

various feedback and feed-forward mechanisms must provide specificity and sensitivity on the post-transcriptional level.

One of the cellular differentiation processes with important implications on overall human health is adipogenesis. Unbalanced energy homeostasis is directly connected to the volume and endocrine signaling of the adipose tissue.[13] At high excess energy intake the subcutaneous and, more importantly, the abdominal fat deposits expand acquiring different problematic characteristics such as altered secretion of adipokines, saturated lipid storage capacity, and flooding of the systemic circulation with free fatty acids, resulting in insulin resistance.[14] The consequences of these systematic fluctuations can come to, among other problems, hypertension, hyperlipidemia, and hyperglycemia, all symptoms of the metabolic syndrome, a condition that is associated with coronary heart disease and increased mortality.[15]

In the early stages of adipogenic commitment, key transcription factors such as CCAAT/enhancer binding proteins β and δ (C/EBPβ and δ) and the glucocorticoid receptor (GR) induce the activation of peroxisome proliferator-activated receptor γ (PPARγ), a nuclear receptor generally referred to as the master regulator of adipogenesis.[16-18] PPARγ, together with its primary target C/EBPα, proceed to guide the cells toward an adipogenic phenotype through activation of target genes. Many of them have been identified by activating PPARγ with its synthetic agonists (thiazolidinediones) that have been used for the treatment of type 2 diabetes.[19] The primary PPARγ targets include many genes important for triglyceride uptake and storage such as *adipocyte protein 2* (*aP2*), *Aquaporin 7* (*Aqp7*), *glycerol kinase* (*GK*), *scavenger receptor* (*CD36*), and *lipoprotein lipase* (*Lpl*), the last encoding an enzyme crucial for hydrolysis of very low density lipoproteins (VLDL) and chylomicrons.[20]

LPL is a 55-kDa glycoprotein, mainly synthesized in parenchymal cells, such as adipose and muscle tissue, and transported to the luminal surface of the surrounding vascular endothelium. The enzyme is active as a non-covalent homodimer and bound to the endothelium via heparin sulfate proteoglycans.[21] LPL-mediated hydrolysis of triglyceride-rich lipoproteins is important for the rapid clearance of post-prandial lipid loads, thereby providing free fatty acids used for storage and energy metabolism and also building material for the high-density lipoprotein (HDL) particles. In addition, LPL transforms large triglyceride-rich lipoproteins into remnant lipoproteins and low-density lipoproteins (LDL).[22] The lipolytic function of LPL is tightly regulated by a number of co-factors. The presence of apolipoprotein C-II in plasma, for instance, is necessary for lipase activation while apolipoprotein C-III is inhibiting its lipolytic activity.[23,24] LPL activity varies greatly between individuals, but the factors influencing LPL expression are incompletely understood. A PPAR response element was identified in the human LPL promoter[25] and polymorphism of PPARγ-2 is accompanied by 20–35% lower plasma LPL activity.[26] In addition, also a sterol regulatory binding element (SREBP) has been identified in the LPL promoter.[27] Moreover, during adipogenesis, LPL can be regulated by insulin at post-transcriptional and post-translational levels.[28]

Consistently, the adipogenic cascade is stringently controlled at the post-transcriptional level. Among other post-transcriptional regulators, miRNAs play a prominent role during adipocyte differentiation. The formation of white adipose tissue in vivo and differentiation of 3T3-L1 adipocytes in vitro both require miRNA expression.[29,30] In addition to promoting differentiation, multiple miRNAs prevent unwanted differentiation and maintain pre-adipocytes. The miR-27 family has been shown to target *Pparg* mRNA in pre-adipocytes, and thereby, its downregulation is necessary for initiating terminal differentiation.[31-33] Similarly, miR-27 family members are drastically reduced in the beginning of osteoblast maturation but are later upregulated through feed-back mechanisms to support osteocyte mineralization,[34,35] suggesting a wider role for miR-27 family in mesenchymal lineage differentiation.

Another miRNA family implicated in mesenchymal differentiation is the miR-29 family. It is dynamically regulated during osteoblastogenic differentiation and shown to primarily affect the expression of multiple collagen genes as well as inhibit osteogenic repressors.[36] The role of miR-29 family members during adipogenesis has not yet been elucidated, although they are expressed at significant levels in the 3T3-L1 adipocyte cell line[37] and other insulin-sensitive tissues where they regulate insulin signaling and become upregulated upon insulin resistance.[38]

In order to further elucidate the dynamic multilevel regulatory events occurring during adipocyte differentiation, we investigated combinatorial miRNA regulation of the *Lpl* gene. We show that *Lpl* can be regulated by two miRNAs, miR-27a and miR-29a, in mouse 3T3-L1 cells and downregulation of these miRNAs during differentiation allows the full extent of PPARγ-driven induction of *Lpl* in adipocytes. Forced expression of both miRNAs in 3T3-L1 adipocytes represses *Lpl* mRNA levels, and importantly, decreases the secreted enzymatically active LPL protein. Based on our newly described interactions and existing literature on multilevel regulation of LPL expression, we construct a quantitative mathematical model of LPL regulation during adipogenesis that can predict the outcomes upon changes in the regulatory edges. The principles of this model could be extended to regulation of other genes under multilevel combinatorial regulation of transcription factors and miRNAs.

Results

Lpl is a putative combinatorial target of miR-27 and miR-29 miRNA families

With the aim to study combinatorial miRNA regulation in differentiating mouse adipocytes, we chose to focus on miRNA families miR-27 and miR-29. Both members of the miR-27 family, miR-27a and miR-27b, have been shown to be abundantly expressed and become downregulated during mouse and human adipocyte differentiation and are capable of inhibiting adipogenic differentiation.[31-33,39,40] Similarly, miR-29 family member miR-29a is abundantly expressed and downregulated in mature human adipocytes.[40] In addition, members of both miRNA families exhibit increased expression levels in different tissues of diabetic rat models and become induced in mouse 3T3-L1 adipocytes at hyperglycemic

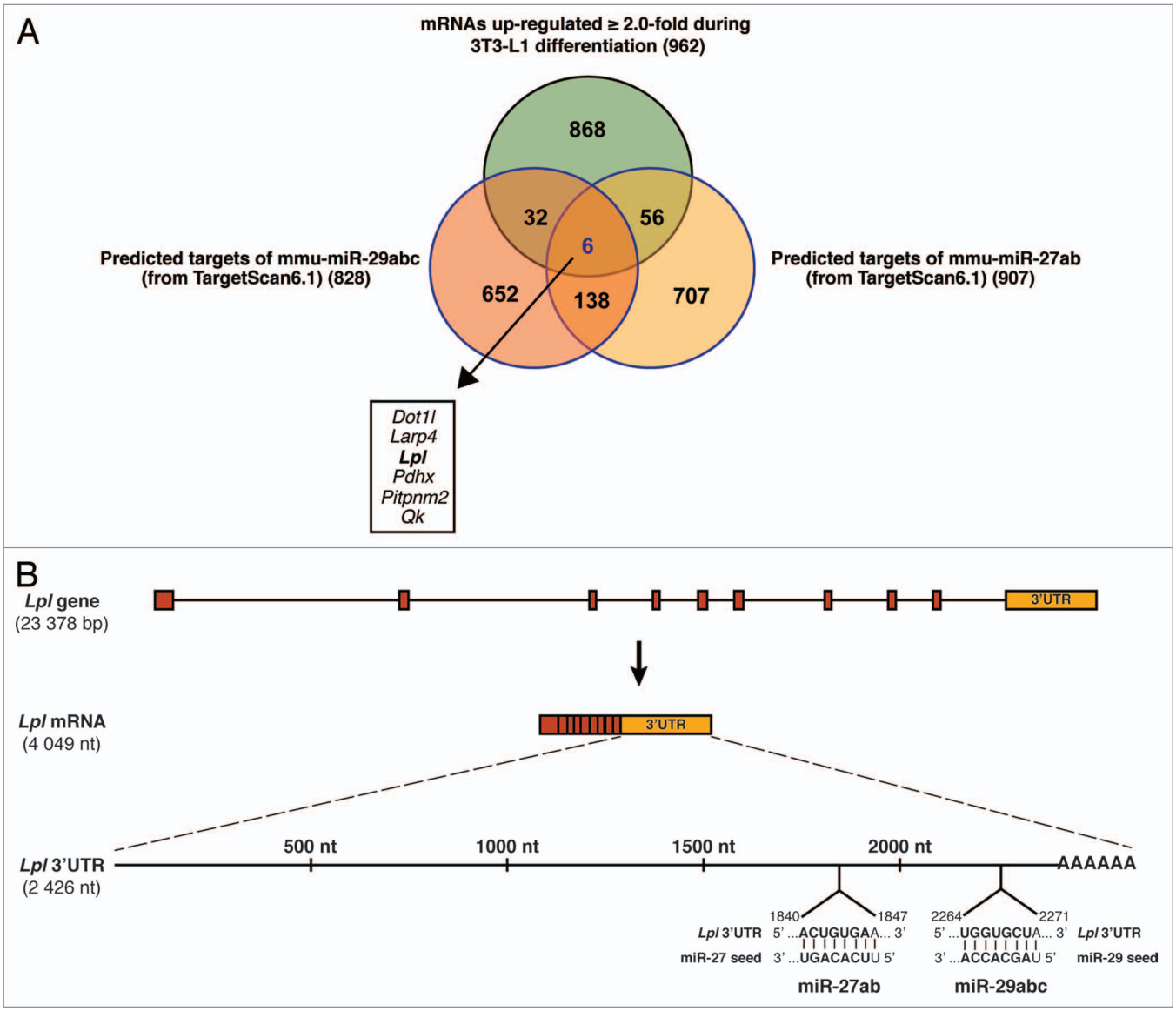

Figure 1. Identifying putative adipogenic target genes for miR-27 and miR-29 families. (**A**) Overlapping gene lists of all putative miR-27 family target genes (907), all putative miR-29 family target genes (828) and ≥ 2-fold upregulated adipogenic mRNA transcripts during 3T3-L1 differentiation[42] reveals 144 shared target candidates between the miRNA families, six of which are induced during differentiation. All predicted target gene lists were generated with TargetScan6.1.[57] (**B**) Gene structure of murine *Lpl* with further overview of the 3′UTR and miRNA-binding seed sites. *Lpl* has an ORF of roughly 4000 nt consisting of nine exons of the coding seqence (red boxes) and a long last exon (orange box) corresponding to the regulatory 3′UTR that constitutes more than half of the mRNA (2426 nt). The miR-27 and miR-29 family 7 nt seed sites are both situated toward the end of the 3′UTR and also carry a complementary A-U base pairing site at the first nt in the 5′-end of the miRNAs.

conditions.[38,41] Taken together, the existing data suggest that both miRNA families could play important roles in insulin-sensitive tissues, and in particular, in adipose tissue.

In order to identify putative shared target genes of the two miRNA families, we obtained lists of predicted conserved targets for the two families from TargetScanMouse6.1. miR-27 and miR-29 are both predicted to target > 700 mRNAs in mouse, 144 of which are potentially shared (**Fig. 1A**). Since miRNAs generally repress their targets and the miRNAs in question are downregulated during adipogenesis, their targets are expected to become upregulated in parallel. To further narrow our list of possible real targets in the adipose tissue, we used publicly available mRNA microarray data for murine 3T3-L1 adipocyte differentiation.[42] Analysis of these data yielded 962 mRNAs showing more than 2-fold upregulation by day 7 of differentiation. Overlapping the predicted shared targets of miR-27 and miR-29 with these upregulated mRNAs identified six putative shared targets of miR-27 and miR-29 in mouse adipocyte differentiation: *Dot1l*, *Larp4*, *Lpl*, *Pdhx*, *Pitpnm2,* and *Qk* (*DOT1-like, histone H3 methyltransferase [S. cerevisiae]*; *La ribonucleoprotein domain family, member 4*; *Lipoprotein lipase*; *Pyruvate dehydrogenase complex, component X*; *Phosphatidylinositol transfer protein, membrane-associated 2*, and *Quaking*, respectively).

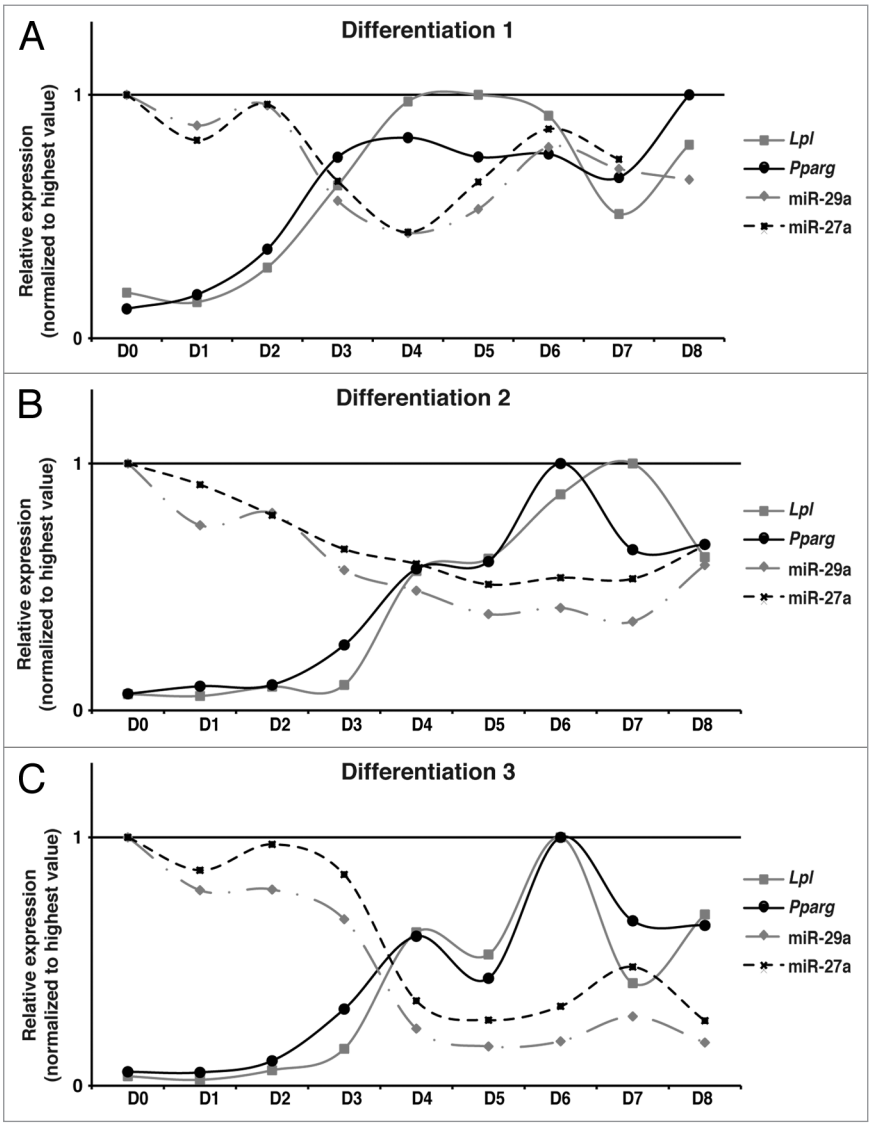

Figure 2. Expression profiles of *Lpl*, *Pparg*, miR-27a, and miR-29a during 8 days of 3T3-L1 mouse pre-adipocyte maturation. The levels of mature mRNAs and miRNAs were quantified with gene specific primers and TaqMan probes, respectively, during induced adipogenesis of 8 d in the mouse 3T3-L1 cell line. (**A–C**) Individual panels depict the relative expression profiles during adipogenesis in three independent differentiation experiments (Differentiations 1–3) for *Lpl*, *Pparg*, miR-27a, and miR-29a. Measured mRNA expression values were normalized to *Rpl13a* mRNA and miRNA values to U6 small nuclear RNA (snRNA) levels. All given data sets are normalized to highest data set value of each sample cohort that is depicted as relative 1.

One of these targets, *Lpl*, the aforementioned critical enzyme for triglyceride uptake, belongs to the cohort of highest induced genes in adipocyte differentiation and is a primary target of PPARγ.[25] Therefore, we chose to focus on *Lpl* for downstream analysis. The predicted binding sites for miR-27 and miR-29 seed sequences are located at the 3′ end of the *Lpl*-3′UTR starting at positions 1840 and 2264, respectively, i.e., some 400 nt apart (**Fig. 1B**).

Taken together, from the 144 predicted shared targets of miR-27 and miR-29, six are upregulated during adipocyte differentiation. In addition, *Lpl*, the most responsive of these targets, is a known primary target of PPARγ, and thereby, also a putative secondary target of miR-27.

miR-27a and miR-29a expression levels are inversely correlated with *Lpl* expression during mouse adipogenesis

miR-27a and miR-27b are transcribed as part of two separate miRNA clusters (miR-23a~27a~24-2 and miR-23b~27b~24-1) located in miRNA genes on chromosomes 8 and 13, respectively. Likewise, there are two different miRNA clusters giving rise to miR-29 family members miR-29a, miR-29b, and miR-29c (miR-29b-1~miR-29a and miR-29b-2~miR-29c) located on chromosomes 6 and 1, respectively. To distinguish which of these miRNA genes are more actively transcribed in pre-adipocytes and affected by transcriptional repression during adipocyte maturation, we analyzed existing ChIP-Seq data of epigenomic characterization of mouse 3T3-L1 adipocyte differentiation (**Fig. S1**).[42] As indicated by the levels of histone modifications like histone H3 lysine 27 acetylation (H3K27ac), a marker for active enhancers, and histone H3 lysine 4 trimethylation (H3K4me3), a marker for transcription start sites, the loci coding for miR-23a~27a~24-2 and miR-29b-1~miR-29a show much more transcriptional activity than the respective loci coding for miR-23b~27b~24-1 or miR-29b-2~miR-29c in pre-adipocytes. Moreover, both loci show some reduction in the histone marks linked to transcriptional activity already at day 2 of differentiation and exhibit clear decrease by day 7. Based on these results, we decided to focus our analysis on clusters miR-23a~27a~24-2 and miR-29b-1~miR-29a, and in particular, on miR-27a and miR-29a as cluster members with unique sequences undergoing downregulation during adipocyte differentiation.

In order to compare the expression dynamics of miR-27a and miR-29a, and their putative targets, we performed three independent differentiation time courses of 3T3-L1 cells and extracted RNA every 24 h (**Fig. 2**). Subsequently, the expression levels of the miRNAs as well as their putative target *Lpl* were analyzed. In addition, we also quantified the expression of *Pparg*, a known target of miR-27a and the main transcriptional regulator of *Lpl* expression. Interestingly, the two miRNAs showed a highly similar expression profile in each differentiation experiment (**Fig. 2**) with only modest or no decrease at the beginning of the differentiation until day 2 and with a stronger reduction from day 3 on down to 15–40% of the original levels in pre-adipocytes, depending on the differentiation. This downregulation appeared dynamic with some increase again toward the end of the time

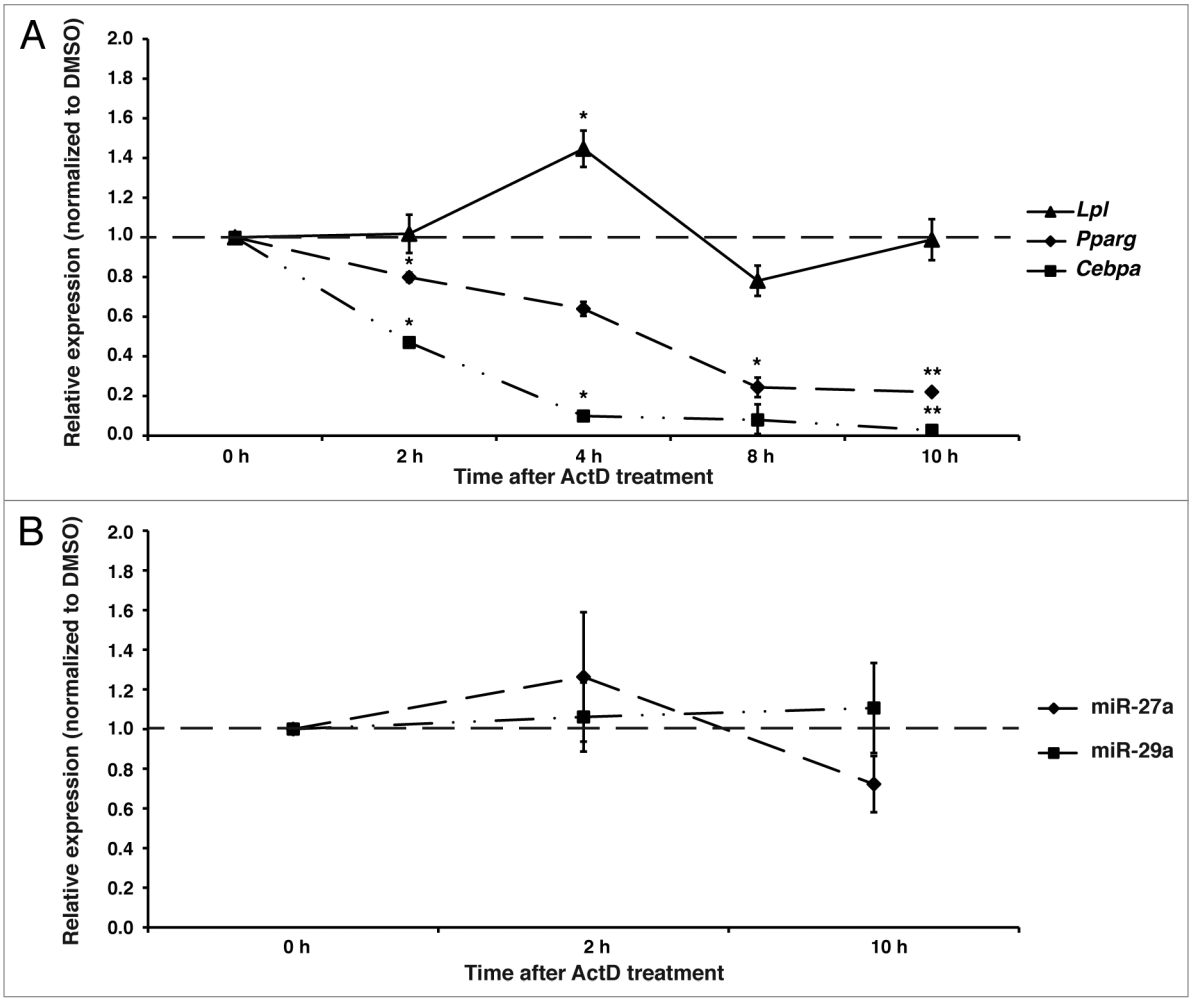

Figure 3. mRNA and miRNA stability in 3T3-L1 pre-adipocytes. Confluent 3T3-L1 pre-adipocytes were treated with ActD on day 0 to inhibit transcription or with DMSO as the vehicle control. Total RNA was harvested after 2, 4, 8, and 10 h of treatment. Levels of (**A**) *Lpl*, *Pparg,* and *Cebpa* and (**B**) miR-27a and miR-29a were quantified by RT-qPCR and normalized to (**A**) *Rpl13a* mRNA levels or (**B**) U6 snRNA levels that were not affected by treatment or vehicle. Each time point value is calculated relative to vehicle DMSO that is set to 1 (indicated by the dashed line). Data indicate the mean expression values of three independent experiments and the error bars represent SEM. One sample *t* test determined the significance of downregulation in response to ActD treatment (*, $P < 0.05$; **, $P < 0.01$).

course. With both miRNAs showing very comparable profiles, it is likely that the expression of these miRNAs is regulated in a highly coordinated manner. However, treating the confluent pre-adipocytes with individual differentiation components alone did not reveal strong downregulation of either of the miRNAs (data not shown), suggesting that they are under combinatorial regulation of multiple factors.

Importantly, also the expression profiles of *Pparg* and its target gene *Lpl* showed similar expression dynamics and inverse expression levels with the tested miRNAs. Both mRNAs showed modest increase until day 2 of differentiation, followed by a stronger induction from day 3 on, and reaching the maximum levels between day 5 and day 6, depending on the differentiation. Moreover, the mRNAs decreased again toward the end of the time course in parallel with the modest increase measured for the miRNAs. The differentiation efficiency was controlled by Oil Red O staining on day 0 and day 8, indicating generally > 90% differentiation efficiency by day 8 of differentiation (**Fig. S2**).

In summary, miR-27a and miR-29a are expressed in a highly coordinated and dynamic manner during mouse adipocyte differentiation and show inverse expression patterns to those of *Pparg* and *Lpl*. This suggests that the miRNAs might serve to prevent an unwanted upregulation of *Pparg* or *Lpl* in pre-adipocytes and regulate their induction during differentiation.

miR-27a, miR-29a, and *Lpl* have long half-lives

In order to better understand the dynamics of the measured miRNAs and mRNAs, we estimated the stability of the tested transcripts. As a control mRNA known to have a short half-life, we included *Cebpa*, another primary target gene of PPARγ coding for an important regulator of adipogenesis.[43] To get an overview of the stability of the miRNAs and mRNAs, transcription in D0 pre-adipocyte cells was blocked by actinomycin D (ActD) for up to 10 h and RNA samples were collected at intermediate

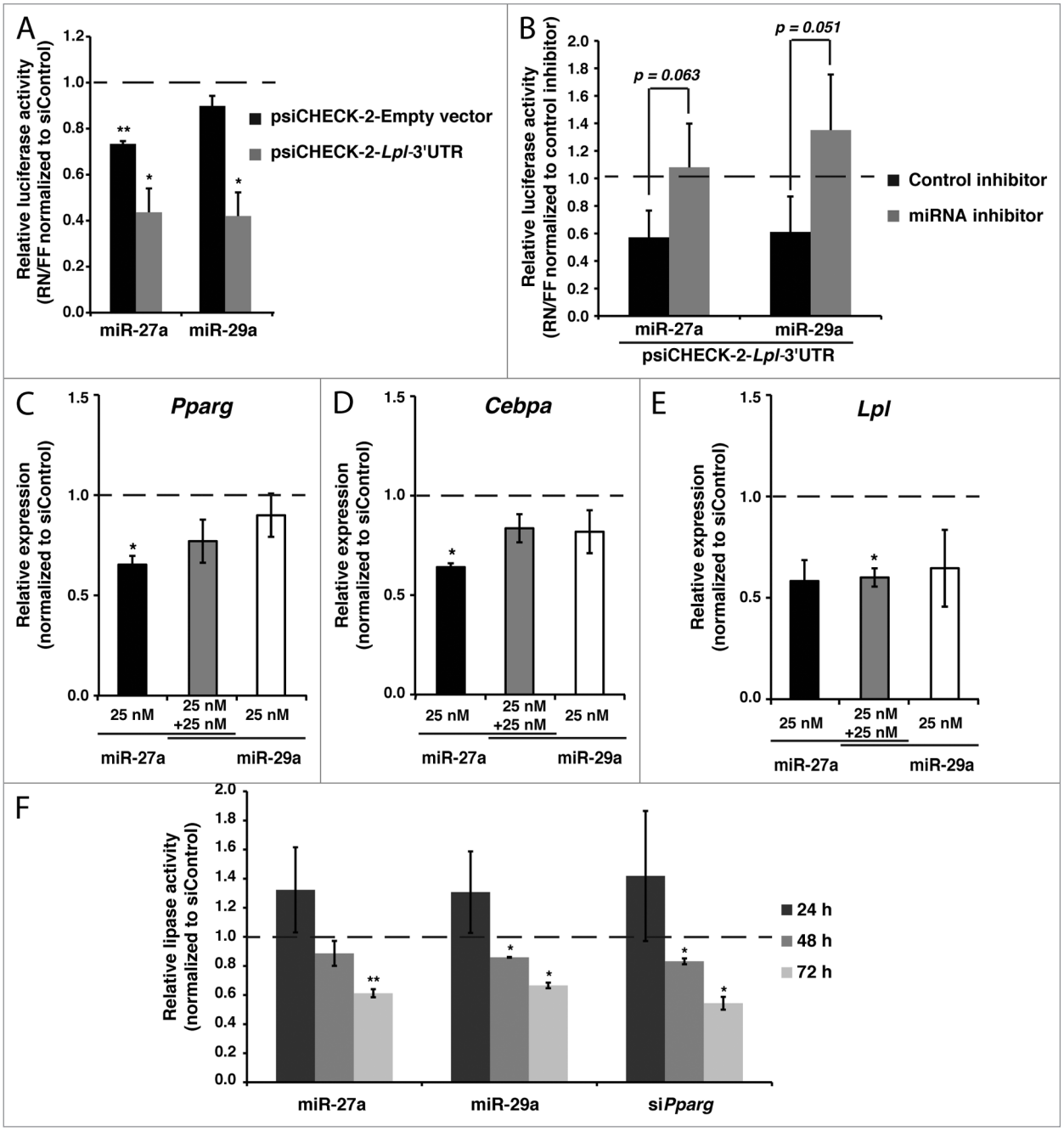

Figure 4. Regulation of *Lpl* and its lipase activity by miR-27a and miR-29a. (**A**) The 3′UTR of the *Lpl* gene was cloned in full-length into the psiCHECK-2 dual-luciferase reporter plasmid immediately downstream of the *Renilla* luciferase reporter gene (psiCHECK-2-*Lpl*-3′UTR). The psiCHECK-2-*Lpl*-3′UTR or empty psiCHECK-2 control vector was co-transfected with 25 nM of miR-27a mimics, miR-29a mimics, or scrambled negative control siRNA (siControl) into HEK293T cells. Cell lysis was performed 24 h after transfection, followed by a quantitative luciferase assay. Data are presented as a ratio of *Renilla* over firefly luciferase, calculated relative to siControl that is set to 1 (indicated by the dashed line). (**B**) The psiCHECK-2-*Lpl*-3′UTR was co-transfected into HEK293T cells as in panel A with 75 nM of scrambled control LNA inhibitor, miR-27a-specific LNA-inhibitor or miR-29a-specific LNA-inhibitor together with 25 nM of miR-27a mimics or miR-29a mimics, respectively. Cell lysis was performed 24 h after transfection, followed by a quantitative luciferase assay. Data are presented as a ratio of *Renilla* over firefly luciferase, calculated relative to LNA-inhibitor alone that is set to 1 (indicated by the dashed line). (**C–E**) Six days differentiated 3T3-L1 cells were transfected with 25 nM of miR-27a mimics, miR-29a mimics, with both miRNAs or with scrambled negative control siRNA (siControl). Cells were harvested 24 h post-transfection and total RNA was extracted. Changes in mRNA expression levels for (**C**) *Pparg*, (**D**) *Cebpa*, and (**E**) *Lpl* were quantified by RT-qPCR. All measured expression values were normalized to *Rpl13a* mRNA and presented as relative to siControl that is set to 1 (indicated by the dashed line). (**F**) Effect of miR-27a and miR-29a overexpression on secreted functional LPL enzyme. Six days differentiated 3T3-L1 cells were transfected with 50 nM miR-27a mimics, miR-29a mimics, scrambled negative control siRNA (siControl), or *Pparg*-specific siRNA (si*Pparg*) that served as a positive control. Medium from transfected samples was collected 24, 48, and 72 h post-transfection and subjected to an LPL enzyme-activity assay. All measured lipase activity values are presented as relative to siControl that is set to 1 (indicated by the dashed line). In all panels the data indicate the mean expression values of three independent experiments and the error bars represent SEM. One sample *t* test (**A and C–F**) or the Student *t* test (**B**) determined the significance of changes in response to miRNA overexpression or their inhibition (*, $P < 0.05$; **, $P < 0.01$; ***, $P < 0.001$).

time points. As previously reported,[44,45] both *Pparg* and *Cebpa* showed a very fast decrease following the ActD treatment with less than 25% of the total mRNA remaining after 8 h and further decreasing by 10 h when compared with the DMSO-treated control samples (**Fig. 3A**). On the contrary, *Lpl* remained at comparable levels to the control samples by the 10 h time point, suggesting a > 10 h half-life for *Lpl* in 3T3-L1 cells.

Similarly to *Lpl*, miR-29a and miR-27a remained largely unaffected after 10 h of transcriptional blocking (**Fig. 3B**), suggesting they possess long half-lives typical for miRNAs. This also fits the dynamics of their downregulation during adipocyte differentiation where they are reduced below 50% only by day 4 of differentiation (**Fig. 2**), although their transcriptional repression is initiated already earlier (as indicated by the epigenetic data and primary miRNA levels; **Fig. S1** and data not shown, respectively).

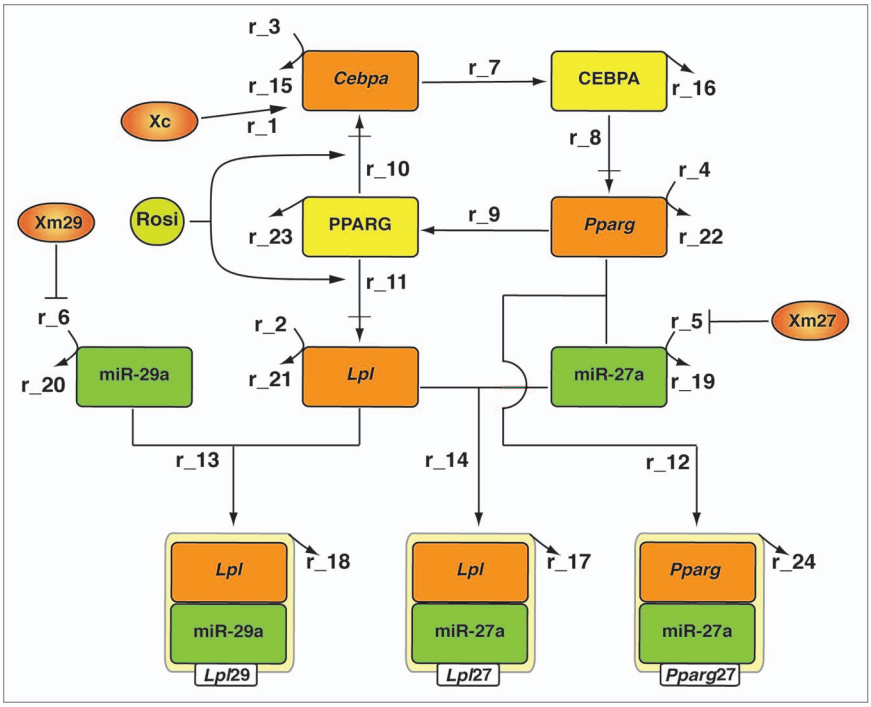

Figure 5. Graphical network representation of the model for LPL regulation. Key components and interactions of the developed ordinary differential equation model depicted in a simplified SBGN notation.[63] The model comprises 10 states, 24 reactions, and 22 parameters. States are represented as rectangles. Yellow background indicates protein (CEBPA, PPARG), orange mRNA (*Cebpa*, *Pparg*, *Lpl*), and green miRNA (miR-27a, miR-29a). The state names were used in the Systems Biology Toolbox2 model (see Supplementary Materials). The variable names of the formed miRNA–mRNA complexes as used in the mathematical model are given in the attached small rectangle. Model inputs (Xc, Xm27, Xm29) are shown as oval shapes where orange-to-yellow gradient background indicates that the exact underlying molecular mechanism is not known or as a green circle (Rosi). Arrows represent reactions with the corresponding reaction name as used in the model. For details on model development, implementation, and model parameters, see Material and Methods and Supplementary Materials.

Lpl-3′UTR mediates the repression by miR-27a and miR-29a

To confirm that *Lpl* mRNA repression by miR-27a and miR-29a can indeed be mediated through *Lpl*-3′UTR, we performed reporter gene assays using a *Renilla* luciferase reporter gene with the complete *Lpl*-3′UTR cloned downstream of the coding sequence in a psiCHECK-2 plasmid (psiCHECK-2-*Lpl*-3′UTR). The psiCHECK-2-*Lpl*-3′UTR, or an empty psiCHECK-2 vector as control, were transfected into HEK293T cells together with miR-27a, miR-29a, or scrambled siRNA as control (siControl). The luciferase activity was measured 24 h post-transfection. As shown in **Figure 4A**, both miR-27a and miR-29a could specifically repress the psiCHECK-2-*Lpl*-3′UTR activity by more than 50% when compared with the cells similarly transfected with siControl. As a side effect, miR-27a had also some repressive effect on the empty vector control while miR-29a affected only the vector with *Lpl*-3′UTR. Nonetheless, inclusion of *Lpl*-3′UTR led to stronger repression by miR-27a, arguing that the repression of the reporter by both of the miRNAs can be mediated through the *Lpl*-3′UTR, while miR-27a can also directly or indirectly repress psiCHECK-2 basal expression. Similar results were also obtained using HeLa cells (data not shown).

Moreover, to further test the specificity of the targeting of *Lpl*-3′UTR by the miRNAs, we performed the co-transfections again in the presence of complementary miRNA-specific LNA-inhibitor molecules, or a scrambled control inhibitor. Importantly, both miRNAs were able to repress the reporter containing *Lpl*-3′UTR in the presence of the control LNA-inhibitor to similar extent as above, but this repression was fully abolished in both cases by the inclusion of the miRNA-specific inhibitors (**Fig. 4B**). Thus, based on these results, both miR-27a and miR-29a are capable of repressing *Lpl*, and this repression is mediated through *Lpl*-3′UTR.

Effect of miR-27a and miR-29a overexpression on *Pparg*, *Cebpa*, and *Lpl* during 3T3-L1 adipogenesis

To investigate the effect of the miRNAs on the endogenous mRNAs of *Pparg*, *Cebpa*, and *Lpl* in differentiating adipocytes, overexpression experiments were performed in adipocytes. Six days differentiated 3T3-L1 adipocytes were transfected with either of the individual miRNA mimics or combinatorially with the two miRNA mimics and harvested 24 h post-transfection. SiControl-transfected cells served as a control. As depicted in **Figure 4C**, miR-29a had no effect on the levels of the endogenous *Pparg*, while miR-27a had a significant effect of approximately 40% decrease in *Pparg* levels. This is consistent with previous reports that *Pparg* is a primary target of the miR-27 family.[31-33] In keeping with the fact that *Cebpa* is a primary target of PPARγ and highly dependent on its transcriptional activity, *Cebpa* was also significantly downregulated upon miR-27a overexpression but remained at elevated levels upon miR-29a overexpression (**Fig. 4D**).

Overexpression of both miR-27a and miR-29a caused some downregulation of *Lpl* mRNA already 24 h post-transfection,

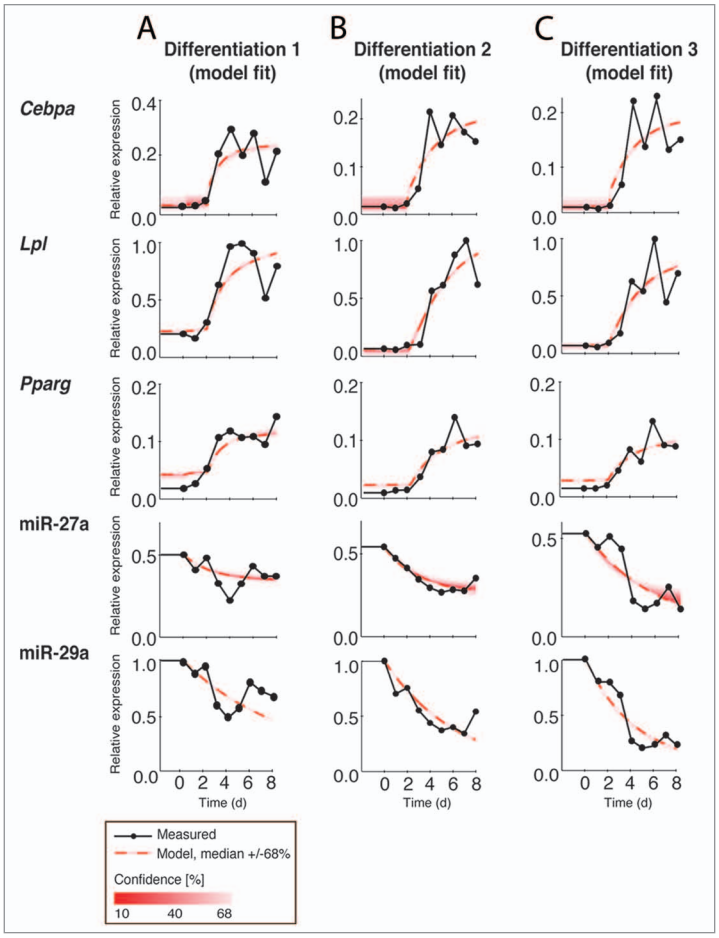

Figure 6. Fitting the mathematical model parameters to the three 3T3-L1 differentiation time courses. Model fit for three independent adipogenic differentiation time courses (see **Fig. 2**) and five model states resulting from parameter identification in Systems Biology Toolbox2 that combined global and local parameter estimation algorithms. Black dotted line represents measured mRNA levels and red dashed line represents the median of all iterations of the model fit within an optimal cost threshold of 1.33-fold of the best obtained fit with red solid lines fading up to 68% confidence. Measured mRNA expression values are normalized to highest mRNA data point and measured miRNA expression values are normalized to highest miRNA data point. All axes and data points correspond to measured cDNA ratios.

with the most significant repression occurring upon equimolar combinatorial transfection of both miRNAs (**Fig. 4E**). The exact extent of the mRNA repression could depend on the differentiation level of the transfected cells. Indeed, the repression of *Lpl* by miR-29a varied considerably between experiments with some showing 2–3-fold stronger repression than others, effectively causing unusually high variation at these conditions.

Taken together, both miR-27a and miR-29a are capable of repressing endogenous *Lpl* mRNA levels in 3T3-L1 adipocytes while only miR-27a can repress *Pparg* and thereby indirectly its primary targets.

miR-27a and miR-29a overexpression leads to lowered lipase activity of the adipocyte-secreted LPL enzyme

To confirm that the observed repression of *Lpl* upon increased miRNA levels also leads to repression of lipase activity of the secreted protein, we measured the enzymatic activity of secreted LPL. This was achieved by transfecting 6 days differentiated 3T3-L1 adipocytes with miRNA mimics or siControl and collecting the culture media 24, 48, and 72 h post-transfection for a lipase activity assay. As a positive control we knocked-down PPARγ, which led to a significant decrease in LPL activity already after 48 h of knockdown (**Fig. 4F**). Similarly, the miRNAs had no effect on LPL activity yet at 24 h. But consistently with their direct targeting of *Lpl* mRNA starting from 24 h on, the increased miRNA levels caused a decrease in measured enzymatic activity of the secreted LPL by 48 h, followed by a further significant decrease by 72 h post-transfection. This argues that targeting of *Lpl* by miRNAs miR-27a and miR-29a can lead to lowered functional activity of the LPL enzyme, and are likely to lower triglyceride uptake by the adipocytes. However, further experiments are needed to test the impact of the miRNAs on triglyceride levels of differentiated adipocytes.

Mathematical modeling of the miRNA regulation network of *Lpl*

Summary of the main interactions governing the regulation of *Lpl* in adipocyte differentiation by PPARγ, miR-27a and miR-29a based on the obtained experimental data and literature is depicted as a graphical network representation in **Figure 5**. In this summary, the differentiation initiation by the external signals (Xc) leads to a transcriptional cascade that triggers the expression of CEBPα, which in turn, increases the levels of PPARγ and leads to a regulatory feed-forward loop between the two transcription factors. In parallel, the repression of the two miRNAs, miR-27a and miR-29a, is initiated by for-now-unknown external signals (Xm27 and Xm29), enabling the ongoing upregulation of PPARγ, a primary target of miR-27a. After 2 days of differentiation, PPARγ agonist rosiglitazone (Rosi) is included in the differentiation cocktail, allowing the full extent of PPARγ activation and induction of its target genes. These include *Lpl* that has been expressed at low levels in the pre-adipocytes and targeted to RISC-like complexes by the abundant miR-27a and miR-29a. The concomitant downregulation of the miRNAs allows for strong upregulation of *Lpl* and proper establishment of the adipogenic phenotype.

To investigate if the obtained experimental data are already sufficient to generate a consistent and quantitative description of the overall behavior of the system, a small mathematical model was developed comprising the key elements and interactions. The model parameters were fitted to the experimental data. The main questions to be answered with the model are, if (1) such a simple principal model allows capturing the key dynamics of miRNA degradation and expression onset, (2) which network structures are responsible for the observed switching behavior, and (3) to carve out the specific characteristics of the individual time courses. Thereby, we focused especially on differentiation 1, which shows a sharper onset and the identification of the potentially responsible parameters. See the Materials and Methods section, as well as Supplementary Materials for details

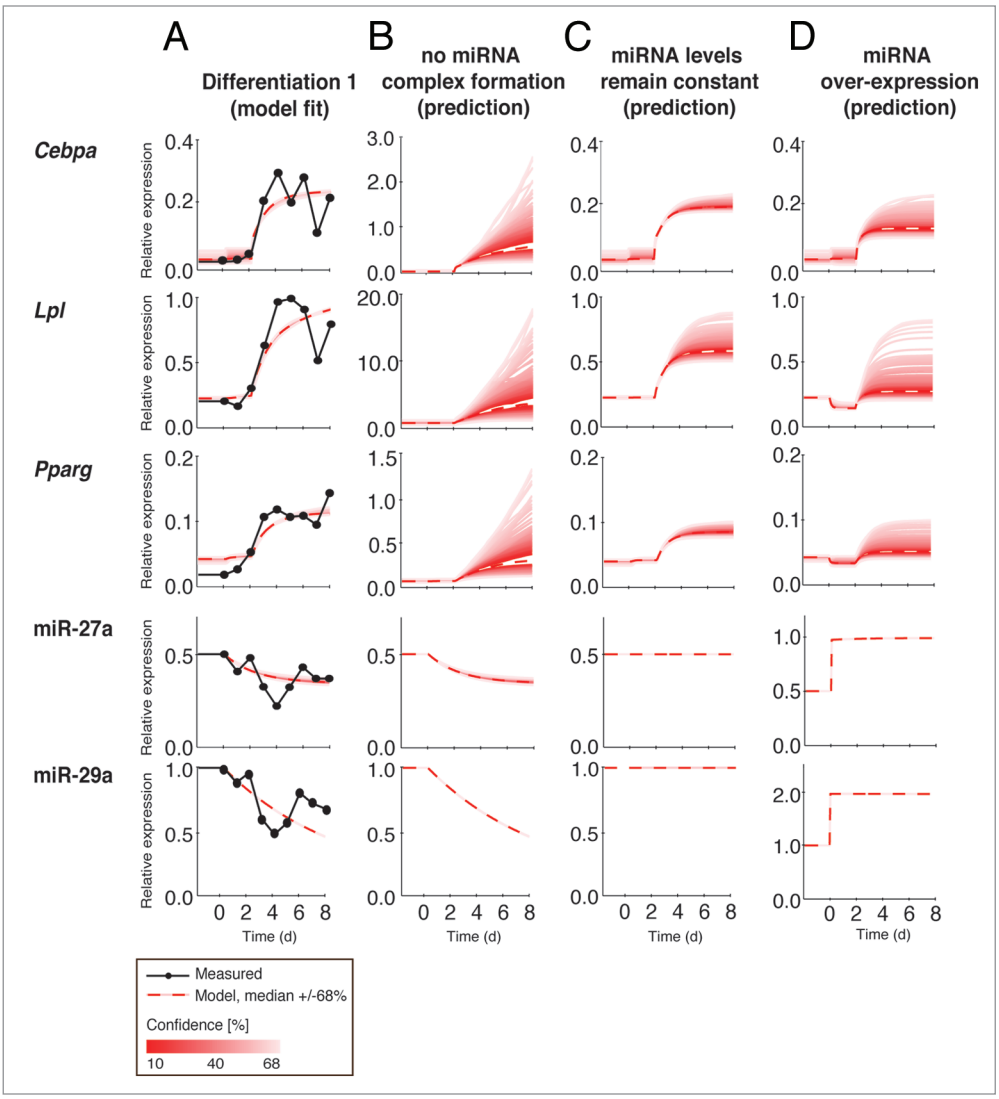

Figure 7. In silico model predictions of target mRNA level changes in response to miRNA perturbation during Differentiation 1. (**A**) The fitted model predicts (**B**) overexpression of *Cebpa*, *Lpl,* and *Pparg* when miRNA-target complexes are not forming; (**C**) downregulation of *Cebpa*, *Lpl,* and *Pparg* when miRNA levels remain at Day 0 levels; (**D**) and strong reduction in *Cebpa*, *Lpl,* and *Pparg* levels (up to 80% for *Lpl*) when both miRNAs miR-27a and miR-29a are 2-fold overexpressed at differentiation start. Black dotted line represents measured mRNA levels and the red dashed line represents the median of all iterations of the model fit within an optimal cost threshold of 1.33-fold of the best obtained fit, respectively, the median of the predictions obtained by using these selected model fits, with red fading up to +/–68% of confidence levels. Measured mRNA expression values are normalized to highest mRNA data point and measured miRNA expression values are normalized to highest miRNA data point. All axes and data points correspond directly to measured cDNA ratios. Confidence intervals are 68% for shown fits.

on modeling, parameter estimation, and in silico predictions. As the three measured differentiation time courses showed some differences in their dynamics, the mathematical model was fitted to all of them independently (**Fig. 6**). Only a subset of the unknown parameters, (nine out of 22) have a low relative standard deviation (≤ 30%) and can therefore be considered to be practically identifiable (**Table S3**). Most other parameters (exceptions discussed below) have the same mean across the three experiments but with a higher relative standard deviation.

Fits were obtained for three experiments, indicating that this simple principal model already allows capturing the key dynamics of the investigated network, i.e., downregulation of the miRNAs and fast onset of the mRNA expression. This switch-like nonlinear behavior is due to the positive feedback loop linking PPARγ and C/EBPα. Differentiation 1 shows a sharper onset (**Fig. 6A**) compared with the other two differentiations (**Fig. 6B and C**), which is also captured by the mathematical model. The basal mRNA production rates of *Pparg* and *Cebpa*, as well as the miRNA–mRNA complex formation rate constants, were estimated to be significantly higher than in the other two time courses (**Table S3**). The increased basal expression of the *Pparg* and *Cebpa* requires a higher miRNA complex formation already in the unstimulated system and forms a system under tension, which acts faster once the miRNA levels are decreasing. This predicted higher basal mRNA expression for differentiation 1 was confirmed by RT-qPCR (data not shown).

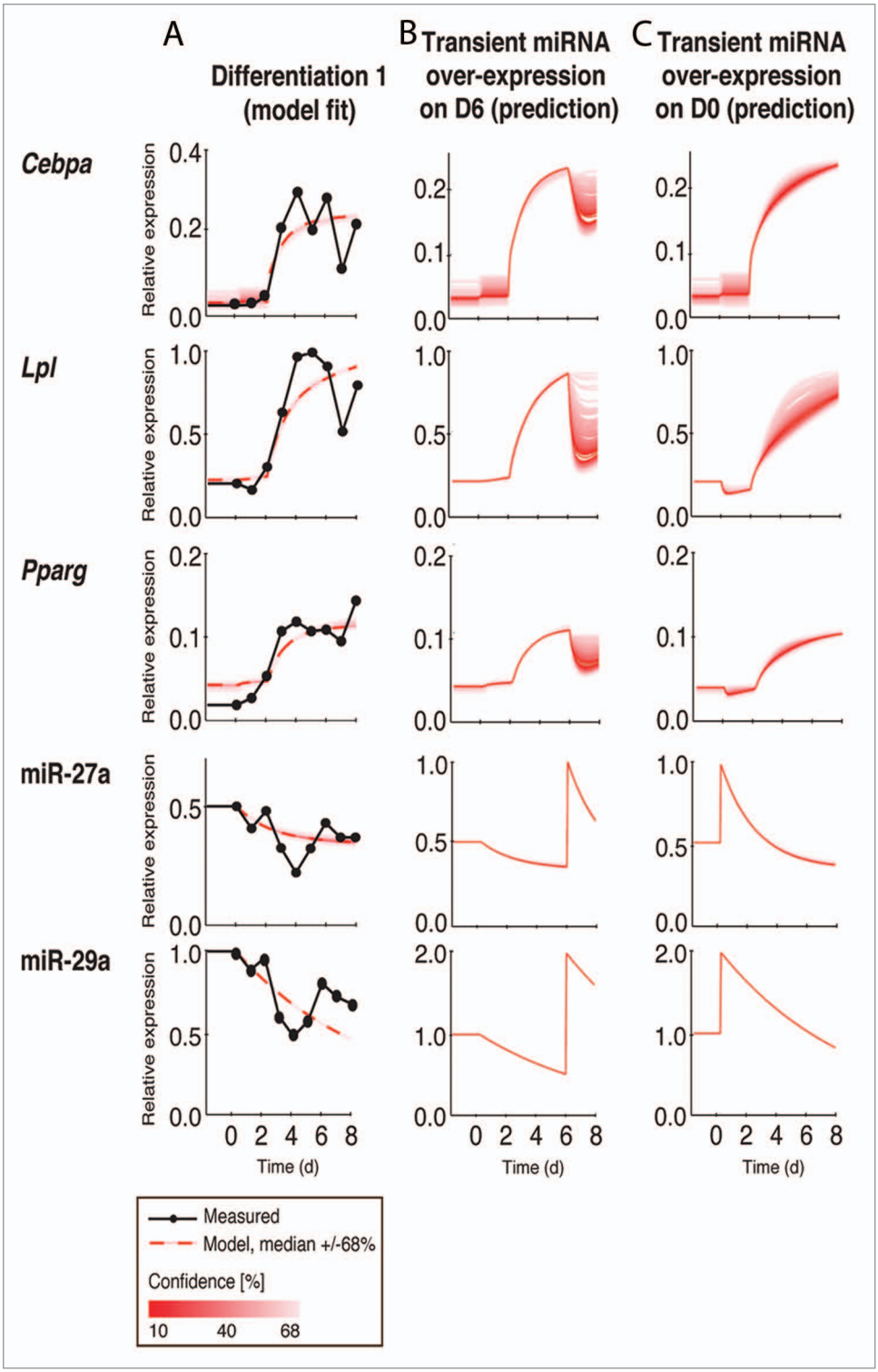

Figure 8. In silico model predictions of target mRNA level changes in response to transient miRNA over-expression during Differentiation 1. (**A**) The fitted model (**B**) predicts up to 60% reduction in *Lpl* levels and around 40% reduction in *Cebpa* and *Pparg* levels when both miRNAs are transiently 2-fold overexpressed at D6. (**C**) No significant effect on *Cebpa* or *Pparg* levels is predicted when both miRNAs are 2-fold overexpressed at differentiation start, while *Lpl* is modestly repressed and delayed in its response. For further details, see **Figures 7 and 9.**

Using this established model, further in silico investigations and predictions were performed by simulating the effects of disabling miRNA–mRNA complex formation, of keeping the miRNA levels constant, and of overexpressing miRNAs 2-fold (**Fig. 7**; **Figs. S3 and S4**). Disabling miRNA complex formation results in an increased and more rapid induction of *Cebpa*, *Lpl,* and *Pparg* mRNAs during differentiation (**Fig. 7B**; **Figs. S3B and S4B**), while stable or overexpressed miRNA levels result in slower and decreased mRNA upregulation (**Fig. 7C and D**; **Figs. S3C and D, S4C and D**). Interestingly, in each case the model predicts only an altered robustness in the response of *Lpl* without fully preventing or releasing its expression. All three differentiations show this same qualitative behavior, although the effect is more pronounced for the model based on differentiation 1, as the system under tension is more dependent on the miRNAs (**Fig. 7**).

Validation of the model predictions for stable overexpression or complete deletion of miRNA function would require the establishment of sophisticated cellular systems where the levels of the different molecules can be accurately controlled. To circumvent this issue, we instead predicted the impact of a transient combinatorial miRNA overexpression on D6 of differentiation (**Fig. 8**), similarly to the experiment depicted in **Figure 4C–E**. Interestingly, the model predicted a clear reduction in the levels of all three tested mRNAs in response to the increased miRNA levels. The predicted reductions were somewhat stronger but comparable to those previously obtained experimentally on day 7 of differentiation, when the target mRNAs are highly expressed (**Fig. 8B**). Also, the model was accurately predicting the effect to be stronger on *Lpl* than on *Pparg* or *Cebpa*.

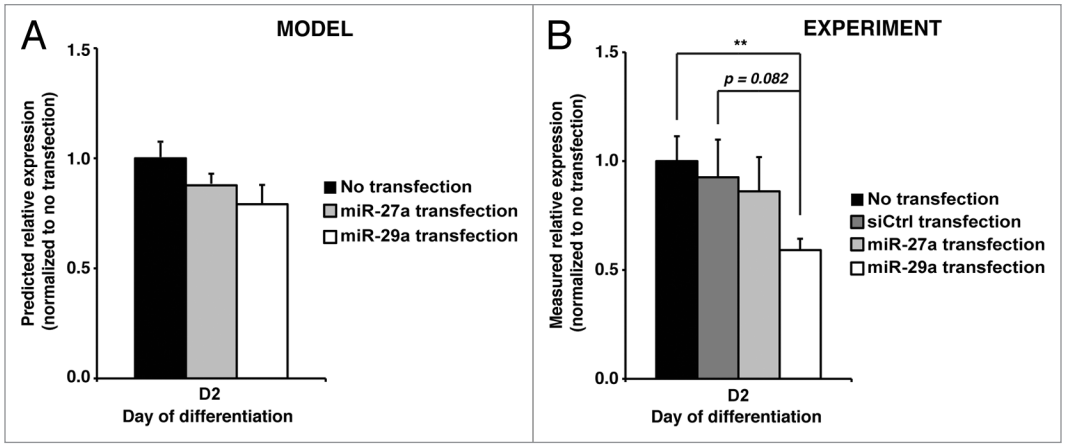

Figure 9. In silico model predictions and experimental validation of *Lpl* mRNA level changes in response to transient overexpression of individual miRNAs prior to differentiation onset. (**A**) A bar graph presentation of the in silico predicted relative *Lpl* expression values for the time point D2 upon overexpression of either miR-27a or miR-29a. Error bars represent upper and lower bounds of the 68% confidence interval of the predictions. (**B**) The level of *Lpl* mRNA was quantified with gene-specific primers on time point D2 of adipogenesis induced in the mouse 3T3-L1 cell line following either a transient transfection of 25 nM siControl, miR-27a mimic, miR-29a mimic, or no transfection. Measured expression values were normalized to *Rpl13a* mRNA and presented as relative to no transfection control that is set to 1. The data indicate the mean expression values of three independent experiments and the error bars represent SEM. One sample *t* test determined the significance of changes in response to miRNA overexpression (**, $P < 0.01$).

Encouraged by these results, we set out to test what kind of an effect similar transient overexpression of the miRNAs might have on the target mRNAs and differentiation when performed on day 0, before differentiation onset. In contrast to stable overexpression depicted in **Figure 7D**, the model predicted only weak or no downregulation for *Pparg* and *Cebpa*, at the beginning of the differentiation, which largely disappeared by the end of differentiation, consistent with the transient nature of the overexpression (**Fig. 8C**). In case of *Lpl*, the initial downregulation was predicted to be slightly stronger and the delayed and reduced induction was maintained also later.

To study the predicted modest impact on *Lpl* more closely and test this prediction experimentally, the model was used to predict in silico the impact of the individual miRNAs on *Lpl* upon transient overexpression on day 0 (**Fig. 9**). As shown in **Figure 9A**, both miRNAs were predicted to be capable of reducing *Lpl* levels by day 2, with miR-29a showing a slightly stronger effect than miR-27a. To see if similar results could be obtained in vitro upon transient miRNA overexpression, the 3T3-L1 cells were transfected on day 0 prior to differentiation and *Lpl* mRNA levels were measured on day 2 of differentiation (**Fig. 9B**). While fairly weak, a qualitative behavior of *Lpl* similar to the in silico predictions could be observed following the overexpression of the individual miRNAs. Again, miR-29a exhibited a stronger effect while the effect of miR-27a was within experimental variation (**Fig. 9B**). However, at later time points, the *Lpl* levels in miRNA-transfected cells reached those of the control cells and the overall differentiation was not inhibited (**Fig. S5**). This was also confirmed by Oil Red O staining of the differentiated transfected cells, which appeared comparable to the control cells in their lipid accumulation (data not shown).

Taken together, this integrated modeling shows that the collected literature information and experimental data allow generation of a consistent representation of the underlying molecular network, in terms of a mathematical description. The fitted and predicted dynamical behavior matches the current knowledge, including many of the experimental results here, although more data needs to be incorporated in order to get a fully identifiable model with higher prediction confidence. The mathematical model therefore is a good starting point for planning further experiments.

Discussion

LPL is a key player in the metabolism of neutral lipids and plays an important role in providing triglyceride components to various cells. It is also central for successful adipogenesis and for maintaining adipose tissue, an organ that is often mistaken as a simple storage of lipids. This misconception was unraveled stepwise when the transcription factors governing adipogenesis were uncovered.[46] Several decades of research have been dedicated to studying function and regulation of LPL, but its exact regulation in health and disease remains to be elucidated in detail. The lack of knowledge is reflected by the continuous debate whether or not LPL is pro- or anti-atherogenic and under what circumstances.[47] In addition, LPL has been targeted by several drugs to treat either lipid disorders (PPARα agonists), or is affected by the glucose-lowering anti-diabetic thiazolidindiones (PPARγ agonists).[48] All of these attempts, however, yielded mixed results in clinical practice, likely due to missing information about the versatile function of LPL in cells that were not the primary target of the drugs.[49,50]

Various factors complicate the issue, such as the cell-autonomous role of LPL, the complex and partly juxtaposed enzymatic and non-enzymatic functions of LPL, and the combination of both transcriptional and post-transcriptional regulation of the molecule.[47] In addition to its regulation by transcription factors like PPARγ, LPL is recognized as

regulated at the post-transcriptional level, a fact reflected also by the particularly long 3′UTR of *Lpl* (**Fig. 1B**). Indeed, already more than two decades ago it was suggested that while LPL upregulation during adipocyte differentiation is driven especially by increased transcription, its activation by insulin is mainly dependent on post-transcriptional activation.[28] In line with this observation, later work has shown that LPL becomes downregulated in the adipose tissue of diabetic rats at the post-transcriptional level and this downregulation depends on specific regions of *Lpl* 3′UTR.[51] It is therefore conceivable that miRNAs, which have emerged as the major post-transcriptional regulators of most mammalian mRNAs, are also targeting *Lpl*. Indeed, recent studies have separately presented miR-467b and miR-29a as single regulators of *Lpl* in steatosis-induced hepatocytes and dendritic cells, respectively.[52,53] Here we show that miR-27a and miR-29a clearly determine LPL expression and activity in adipocytes and demonstrate that both miRNAs act in a combinatorial fashion. Interestingly, both miR-27a and miR-29a are also among the few miRNAs upregulated in adipocytes of diabetic rats,[38,41] suggesting that they could play a role in the above mentioned decrease of LPL in diabetes.

In addition to targeting *Lpl*, miR-27a also represses the expression of PPARγ, the key transcriptional regulator of *Lpl*. In this way they constitute a coherent feed-forward loop where the miRNA regulates multiple transcripts along the same regulatory axis and leads to a delay in the response upon a dynamic shift.[54] In order to provide a more systematic overview or simulation of various combinatorial factors, we took advantage of a systems biology approach of constructing a small mathematical model that could be helpful in determining LPL regulation under different circumstances and in different target organ systems. Our model was able to capture the key dynamics of the studied network and allowed the prediction of the effects of elaborate perturbations in the network. Interestingly, predicting the effect of no downregulation or even upregulation of miRNA levels during adipogenesis led only to decreased and delayed response of *Lpl*, and not to a fully inhibited induction, according to the model. This is consistent with the general role of type 2 coherent feed-forward loops in delaying the target response,[54] and with the proposed role for miRNAs in buffering the levels of their target mRNAs during cell state transitions.[55]

Curiously, the results from in silico predictions upon transient miRNA overexpression suggest that, while efficient in reducing the target mRNAs in differentiated adipocytes, the impact remains modest when overexpressed in pre-adipocytes—an observation that was also confirmed experimentally (**Figs. 4C–E, 8, and 9**). A possible explanation could be that in pre-adipocytes the expressed target mRNAs are already occupied by the abundant endogenous miRNA-complexes, and strong additional repression of the target mRNAs is not possible.

In addition to modeling *Lpl* regulation, our model can be extended and modified to analyze other similar network motifs. For example, miR-27 family is establishing itself as one of the key regulators of lipid metabolism and seems to be targeting multiple enzymes along the triglyceride synthesis pathway, in addition to LPL.[40,56] In the future, combining this type of small models of miRNA regulatory networks with large scale metabolic modeling might enable predicting the impact of miRNAs on the cellular metabolism more accurately.

Materials and Methods

Identification of putative combinatorial targets of mir-27 and miR-29 families in mouse 3T3-L1 adipocytes

MiRNA target predictions for miR-27 and miR-29 families were obtained from TargetScanMouse (Release 6.1)[57] and all target mRNAs with at least one conserved binding site were included in the analysis. A publicly available microarray data set of transcriptomic changes during three time points (day 0, 2, 7) of mouse 3T3-L1 adipocyte differentiation[42] was used to identify the mRNAs with at least one probe set upregulated above 2-fold by day 7 of differentiation.

Cell culture

The murine pre-adipocyte cell line 3T3-L1 was obtained from ATCC and maintained in Dulbecco's modified Eagle-medium supplemented with 10% fetal calf serum (Gibco, 10270-106), 1% penicillin–streptomycin, and 1% L-glutamine (Lonza, DE17-602E, BE17-605E). The cells were kept at 37 °C and 5% CO_2. Pre-adipocytes were differentiated into mature, fat-storing adipocytes as previously described.[58] Please note that rosiglitazone, which is included in the differentiation cocktail from D2 on, can lead to some browning of 3T3-L1 adipocytes,[59] and thus, the presented results may also be true for brite mouse adipocytes. In order to stain the lipids in pre-adipocytes and adipocytes, Oil Red O solution (Sigma-Aldrich) was used. Briefly, day 0 and day 8 adipocytes were fixed in 10% formalin and incubated for 10 min at room temperature. Then formalin was removed and renewed with fresh formalin for at least 1 h. Again formalin was removed and adipocytes were rinsed with 60% isopropanol and dried. Then Oil Red O solution was added to adipocytes and incubated during 10 min at room temperature. Finally Oil Red O solution was removed, adipocytes were rinsed with H_2O and imaged. For ActD treatment, the cells were grown to confluency and at day 0 treated with 2 µg/ml ActD or an equal volume of vehicle control (dimethyl sulfoxide [DMSO]). The human embryonic kidney 293T (HEK293T) cell line was maintained in RPMI 1640 medium supplemented with 10% fetal calf serum, 1% penicillin–streptomycin, and 1% L-glutamine and kept at 37 °C and 5% CO_2.

miRNA transfections and RNA interference

MiRNA mimics for miR-27a and miR-29a (Thermo Scientific Dharmacon, C-310523-05-0005, C-310521-07-0005) and a scrambled double-stranded siRNA sequence as control (siControl) (Eurogentec, SR-CL000-005) were introduced into undifferentiated 3T3-L1 pre-adipocytes prior to differentiation using Lipofectamine 2000 (Invitrogen, 11668-019) according to the manufacturer's instructions. MiRNA mimics for miR-27a and miR-29a, gene-specific siRNAs against mouse *Pparg* (si*Pparg*) (Thermo Scientific Dharmacon, C-310523-05-0005, C-310521-07-0005), and a scrambled double-stranded siRNA sequence as control (siControl) (Eurogentec, SR-CL000-005) were introduced into 6 days differentiated 3T3-L1 adipocytes using Nucleofector

II Device (program A-033) and the Cell Line Nucleofector Kit L (Lonza, VVCA-1005 KT) according to the manufacturer's instructions. The sequences of the siRNAs are listed in **Table S1**.

Luciferase reporter assays

The full-length wild-type murine 3′untranslated region (3′UTR) of the *Lpl* gene was synthesized and cloned into the psiCHECK-2 vector (Promega) at XhoI/NotI sites downstream of *Renilla* luciferase translational stop codon (DNA2.0 Inc.). Empty psiCHECK-2 vector served as a control plasmid.

For the 3′UTR reporter assay, ~90% confluent HEK293T cells were co-transfected with 25 nM miR-27a or miR-29a mimics or siControl and 200 ng of either of the psiCHECK-2 constructs in 12-well plates with Lipofectamine 2000 (Invitrogen, 11668-019). Twenty-four hours post-transfection, the cells were washed with 500 µl of PBS and lysed in 250 µl of passive lysis buffer. Ten µl of the lysate was used for measuring the *Renilla* (RL) and firefly (FL) luciferase activities in a FluoStar Optima instrument (BMG LABTECH) using the Dual-Luciferase Reporter Assay System (Promega, E1960) according to manufacturer's instructions. Samples were quantified in technical duplicates on a 96-well plate. Each condition was performed in technical duplicates and in three biological replicates. The specific RL activity was normalized to the respective FL activity.

miRNA inhibitor transfections

MiRNA mimics for miR-27a and miR-29a (Thermo Scientific Dharmacon, C-310523-05-0005, C-310521-07-0005) together with their respective inhibitor, miR-27a LNA inhibitor (Exiqon, 410168-00), or miR-29a LNA inhibitor (Exiqon, 410174-00), or a scrambled double-stranded negative LNA control (Exiqon, 199020-00) were introduced together with 200 ng of the psiCHECK-2-*Lpl*-3′UTR vector into ~90% confluent HEK293T cells in 12-well plates using Lipofectamine 2000 (Invitrogen, 11668-019) according to the manufacturer's instructions. miRNA mimics were of a final concentration of 25 nM, miRNA inhibitors and the control LNA-inhibitor were of a final concentration of 75 nM. Cells were lysed 24 h after transfection and the lysate used for the Dual-Luciferase Reporter Assay System (Promega, E1960) as described above. Bioluminescence was quantified in a BioTek SynergyMX instrument (BioTek Instruments Inc.).

RNA extraction and cDNA synthesis

3T3-L1 cells were lysed in 1 ml/10 cm^2 TRIsure reagent (Bioline, BIO-38033) on 6-well culture plates. Total RNA was extracted with 200 µl of chloroform, precipitated with 400 µl of isopropanol overnight at -20 °C, ethanol-washed and pelleted by centrifugation. RNA purity and concentration were measured on a NanoDrop2000 spectrophotometer (Thermo Scientific Dharmacon). cDNA synthesis was performed with 1 µg of total RNA and 0.5 mM dNTPs, 2.5 mM oligo-dT primer, 1 U/ml RiboLock RNase Inhibitor (Fermentas, EO0384), 10 U/ml M-MuLV Reverse Transcriptase (Fermentas, EP0352) for 1 h at 37 °C. cDNA synthesis was terminated by 10 min incubation at 70 °C and cDNA diluted to final volume of 400 µl. Please note that the total RNA samples used for the time course results presented in **Figure 2** are same as those used by John et al.[58] and can therefore be compared with results presented there for other miRNA genes.

Quantitative PCR

Real-time quantitative PCR (qPCR) was performed in an Applied Biosystems 7500 Fast Real-Time PCR System using Absolute Blue qPCR SYBR Green Low ROX Mix reagent (Thermo Fisher Scientific, AB-4323/D). Each 20 µl of PCR reaction comprised 5 µl of cDNA template, 5 µl primer pairs (2 µM), and 10 µl of qPCR SYBR mix. The PCR reaction started with 15 min at 95 °C to activate the polymerase and was followed by 40 cycles of 15 s at 95 °C, 15 s at 55 °C, and 30 s at 72 °C. Post-PCR melt curve analysis was used to control the PCR product specificity. Relative expression levels were calculated from raw signal intensities within each independent experiment using the equation $2^{-(\Delta\Delta Ct)}$, where $\Delta\Delta Ct$ is $(Ct_{(target\ gene)} - Ct_{(control\ gene)})_{tested\ condition} - (Ct_{(target\ gene)} - Ct_{(control\ gene)})_{control\ condition}$ and Ct is the cycle at which a user-defined signal threshold is crossed. *Rpl13a* gene was used as the stable control gene and D0, vehicle control or siControl served as control condition. The sequences of the primer pairs are listed in **Table S2**.

miRNA assays

Mature miRNA sequences were selectively reverse transcribed using the TaqMan MicroRNA Reverse Transcription Kit (Applied Biosystems, 4366596) and the expression of mature miRNA transcripts was quantified with the TaqMan MicroRNA Assays (Applied Biosystems, 4440040). All reactions were performed according to the manufacturer's instructions in an Applied Biosystems 7500 Fast Real-Time PCR System. Relative expression levels were calculated within each independent time course experiment using the equation $2^{-(\Delta\Delta Ct)}$, where $\Delta\Delta Ct$ is $(Ct_{(target\ miRNA)} - Ct_{(U6)})_{tested\ condition} - (Ct_{(target\ miRNA)} - Ct_{(U6)})_{control\ condition}$ and Ct is the cycle at which a user-defined signal threshold is crossed. *U6* gene was used as the stable control gene and D0 or vehicle control served as control condition.

LPL enzyme activity assay

Culture medium of day 6 transfected adipocytes was collected 24, 48, and 72 h after transfection and 2 µl of the medium was used to measure LPL activity. The activity of secreted LPL was quantified using the ROAR LPL Activity Assay kit (Roar Biomedical Inc., RB-LPL2) according to the manufacturer's instructions in a BioTek SynergyMX instrument (BioTek Instruments Inc.). Enzymatic activity upon miRNA mimic transfection is presented relative to siControl-tranfected samples.

Mathematical modeling

A small mathematical model using ordinary differential equations (ODEs) was constructed, focusing on the core elements and interactions of the biological system. Based on literature data (and transcription factor binding data), the model comprises as core structures a coherent feed-forward loop, as well as a positive feed-back loop (see **Fig. 5**). The feed-forward loop connects miR-27a to *Pparg* and *Lpl* through translational inhibition and PPARγ to *Lpl* through transcriptional upregulation. PPARγ and C/EBPα are connected through positive feedback on the transcriptional dimension. In addition, miR-29a-dependent translational inhibition of *Lpl* is included, as well as basal production and degradation rates for all mRNAs and miRNAs. Four inputs are used to mimic the experimental procedure, resulting in an increased induction of *Cebpa* transcription from day 0 to day 2 (input Xc), a reduced production of miR-27 from day 0 on (input

Xm27), and a completely abolished production of miR-29 from day 0 on (input Xm29). In addition, rosiglitazone is added at day 2 to activate PPARγ (input Rosi).

Reaction rates were modeled applying the law of mass action. The resulting ordinary differential equation model was implemented in the Systems Biology Toolbox2 within the Matlab© framework.[60] The model comprises 10 states, 24 reactions, and 22 parameters. See Supplementary Materials for the ODE model (parameters and initial conditions from the best fit of differentiation 2) in the unit [1/d] and **Table S3** for details on parameters. miRNA and mRNA half-lives ($t_{1/2}$) were obtained from ActD measurements in D0 pre-adipocytes and additional literature data[43,44] and converted into parameters: $k_{1/2} = \ln 2/t_{1/2}$ (day^{-1}). Consequently, the bounds for these parameters were set according to measured half-lives (**Table S3**). Bounds for unknown parameters were set to (0, 1000). The miR-27 *Lpl* complex (*Lpl*27) formation rate constant was bounded to (0, 10) and other miRNA–mRNA complex formation rates were allowed to deviate from this rate at most 2-fold, to reflect lower miRNA impact compared with other regulations. The effect of internal ligands responsible for the PPARγ activation limited to 50% of the rosiglitazone effect and the production of miR-27 from day 0 on (input Xm27) was estimated between (0, 1), meaning 0–100% of the basal production rate.

All measurements were first normalized to the maximal value. In a second normalization step, the relative (and experiment specific) differences within mRNA and miRNA expressions were taken into account, resulting in different maximal levels for the measured states in the interval (0, 1). Within the model, a 100–1000 fold excess of miRNA over mRNA molecules was assumed. The ratio was consecutively estimated.

The model was fitted for estimating the unknown parameters and initial conditions using measured time course data for *Cebpa*, *Lpl*, *Pparg*, miR-27a, and miR-29a, and a hybrid optimization approach within the Systems Biology Toolbox 2 applying first a global particle swarm algorithm (pswarmSB)[61] followed by a local simplex algorithm (simplexSB).[62] The estimation was initialized with random parameter values (max 2-fold up or down from the initial estimate) within the given bounds 400 times. All fits within an optimal cost threshold of 1.33 times of the best optimal cost were extracted. Median and 68% range (the range captured by one standard deviation in a normal distribution) were plotted with lines indicating 1% steps for the obtained fits and model predictions. In silico predictions were performed based on all parameter sets fulfilling the optimal cost threshold in the respective experiment. For the predictions, miRNA complex formation was inhibited by setting the complex formation rate constants to 0. Stable miRNA levels were modeled by keeping inputs Xm27 = Xm29 = 1 constant and 2-fold overexpression was modeled by changing Xm27 = Xm29 = 2 from day 0 on and adjusting the state value of the miRNAs accordingly.

Disclosure of Potential Conflicts of Interest

No potential conflicts of interest were disclosed.

Acknowledgments

We would like to acknowledge Dr Michele Moes and Dr Evelyne Friederich for sharing the empty psiCHECK-2 vector and Andreas Zimmer, Catherine Rolvering, Demetra Philippidou, Dr Paul Antony, Olga Boyd, and Sandra Köglsberger for the help with reporter gene assays, protein measurements, and cloning.

Funding

This work was supported by funding from the University of Luxembourg and the Fondation National de Luxembourg (Pelican grant for ML by Mie et Pierre Hippert-Faber). M.L. and E.J. were supported by fellowships from the National Research Foundation of Luxembourg (FNR) (AFR 1086506 and AFR 1011788, respectively). J.G.S. was supported by the German Research Association (DFG 682/3-1), the European Union (CIG 303682), and the National Research Foundation of Luxembourg (FNR) (Core 12/BM/3971360).

Supplemental Materials

Supplemental materials may be found here:
www.landesbioscience.com/journals/rnabiology/article/27655/.

References

1. Maston GA, Landt SG, Snyder M, Green MR. Characterization of enhancer function from genome-wide analyses. Annu Rev Genomics Hum Genet 2012; 13:29-57; PMID:22703170; http://dx.doi.org/10.1146/annurev-genom-090711-163723
2. Keene JD. RNA regulons: coordination of post-transcriptional events. Nat Rev Genet 2007; 8:533-43; PMID:17572691; http://dx.doi.org/10.1038/nrg2111
3. Karlebach G, Shamir R. Modelling and analysis of gene regulatory networks. Nat Rev Mol Cell Biol 2008; 9:770-80; PMID:18797474; http://dx.doi.org/10.1038/nrm2503
4. Ghildiyal M, Zamore PD. Small silencing RNAs: an expanding universe. Nat Rev Genet 2009; 10:94-108; PMID:19148191; http://dx.doi.org/10.1038/nrg2504
5. Krol J, Loedige I, Filipowicz W. Regulation of microRNA biogenesis, function and degradation. Nature 2010; 1:20
6. Friedman RC, Farh KK-H, Burge CB, Bartel DP. Most mammalian mRNAs are conserved targets of microRNAs. Genome Res 2009; 19:92-105; PMID:18955434; http://dx.doi.org/10.1101/gr.082701.108
7. Grimson A, Farh KK-H, Johnston WK, Garrett-Engele P, Lim LP, Bartel DP. MicroRNA targeting specificity in mammals: determinants beyond seed pairing. Mol Cell 2007; 27:91-105; PMID:17612493; http://dx.doi.org/10.1016/j.molcel.2007.06.017
8. Saetrom P, Heale BSE, Snøve O Jr., Aagaard L, Alluin J, Rossi JJ. Distance constraints between microRNA target sites dictate efficacy and cooperativity. Nucleic Acids Res 2007; 35:2333-42; PMID:17389647; http://dx.doi.org/10.1093/nar/gkm133
9. Hon LS, Zhang Z. The roles of binding site arrangement and combinatorial targeting in microRNA repression of gene expression. Genome Biol 2007; 8:R166; PMID:17697356; http://dx.doi.org/10.1186/gb-2007-8-8-r166
10. Hornstein E, Shomron N. Canalization of development by microRNAs. Nat Genet 2006; 38(Suppl):S20-4; PMID:16736020; http://dx.doi.org/10.1038/ng1803
11. Mukherji S, Ebert MS, Zheng GXY, Tsang JS, Sharp PA, van Oudenaarden A. MicroRNAs can generate thresholds in target gene expression. Nat Genet 2011; 43:854-9; PMID:21857679; http://dx.doi.org/10.1038/ng.905
12. Stark A, Brennecke J, Bushati N, Russell RB, Cohen SM. Animal MicroRNAs confer robustness to gene expression and have a significant impact on 3'UTR evolution. Cell 2005; 123:1133-46; PMID:16337999; http://dx.doi.org/10.1016/j.cell.2005.11.023
13. Poulos SP, Hausman DB, Hausman GJ. The development and endocrine functions of adipose tissue. Mol Cell Endocrinol 2010; 323:20-34; PMID:20025936; http://dx.doi.org/10.1016/j.mce.2009.12.011

14. Deng Y, Scherer PE. Adipokines as novel biomarkers and regulators of the metabolic syndrome. Ann N Y Acad Sci 2010; 1212:E1-19; PMID:21276002; http://dx.doi.org/10.1111/j.1749-6632.2010.05875.x
15. Malik S, Wong ND, Franklin SS, Kamath TV, L'Italien GJ, Pio JR, Williams GR. Impact of the metabolic syndrome on mortality from coronary heart disease, cardiovascular disease, and all causes in United States adults. Circulation 2004; 110:1245-50; PMID:15326067; http://dx.doi.org/10.1161/01.CIR.0000140677.20606.0E
16. Rosen ED, Sarraf P, Troy AE, Bradwin G, Moore K, Milstone DS, Spiegelman BM, Mortensen RM. PPAR γ is required for the differentiation of adipose tissue in vivo and in vitro. Mol Cell 1999; 4:611-7; PMID:10549292; http://dx.doi.org/10.1016/S1097-2765(00)80211-7
17. Lefterova MI, Steger DJ, Zhuo D, Qatanani M, Mullican SE, Tuteja G, Manduchi E, Grant GR, Lazar MA. Cell-specific determinants of peroxisome proliferator-activated receptor gamma function in adipocytes and macrophages. Mol Cell Biol 2010; 30:2078-89; PMID:20176806; http://dx.doi.org/10.1128/MCB.01651-09
18. Steger DJ, Grant GR, Schupp M, Tomaru T, Lefterova MI, Schug J, Manduchi E, Stoeckert CJ Jr., Lazar MA. Propagation of adipogenic signals through an epigenomic transition state. Genes Dev 2010; 24:1035-44; PMID:20478996; http://dx.doi.org/10.1101/gad.1907110
19. Diamant M, Heine RJ. Thiazolidinediones in type 2 diabetes mellitus: current clinical evidence. Drugs 2003; 63:1373-405; PMID:12825962; http://dx.doi.org/10.2165/00003495-200363130-00004
20. Tontonoz P, Spiegelman BM. Fat and beyond: the diverse biology of PPARgamma. Annu Rev Biochem 2008; 77:289-312; PMID:18518822; http://dx.doi.org/10.1146/annurev.biochem.77.061307.091829
21. Saxena U, Klein MG, Goldberg IJ. Identification and characterization of the endothelial cell surface lipoprotein lipase receptor. J Biol Chem 1991; 266:17516-21; PMID:1654330
22. Goldberg IJ. Lipoprotein lipase and lipolysis: central roles in lipoprotein metabolism and atherogenesis. J Lipid Res 1996; 37:693-707; PMID:8732771
23. Kinnunen PK, Jackson RL, Smith LC, Gotto AM Jr., Sparrow JT. Activation of lipoprotein lipase by native and synthetic fragments of human plasma apolipoprotein C-II. Proc Natl Acad Sci U S A 1977; 74:4848-51; PMID:270715; http://dx.doi.org/10.1073/pnas.74.11.4848
24. Schoonjans K, Peinado-Onsurbe J, Fruchart JC, Tailleux A, Fiévet C, Auwerx J. 3-Hydroxy-3-methylglutaryl CoA reductase inhibitors reduce serum triglyceride levels through modulation of apolipoprotein C-III and lipoprotein lipase. FEBS Lett 1999; 452:160-4; PMID:10386582; http://dx.doi.org/10.1016/S0014-5793(99)00632-8
25. Schoonjans K, Peinado-Onsurbe J, Lefebvre AM, Heyman RA, Briggs M, Deeb S, Staels B, Auwerx J. PPARalpha and PPARgamma activators direct a distinct tissue-specific transcriptional response via a PPRE in the lipoprotein lipase gene. EMBO J 1996; 15:5336-48; PMID:8895578
26. Schneider J, Kreuzer J, Hamann A, Nawroth PP, Dugi KA. The proline 12 alanine substitution in the peroxisome proliferator--activated receptor-gamma2 gene is associated with lower lipoprotein lipase activity in vivo. Diabetes 2002; 51:867-70; PMID:11872694; http://dx.doi.org/10.2337/diabetes.51.3.867
27. Schoonjans K, Gelman L, Haby C, Briggs M, Auwerx J. Induction of LPL gene expression by sterols is mediated by a sterol regulatory element and is independent of the presence of multiple E boxes. J Mol Biol 2000; 304:323-34; PMID:11090277; http://dx.doi.org/10.1006/jmbi.2000.4218
28. Semenkovich CF, Wims M, Noe L, Etienne J, Chan L. Insulin regulation of lipoprotein lipase activity in 3T3-L1 adipocytes is mediated at posttranscriptional and posttranslational levels. J Biol Chem 1989; 264:9030-8; PMID:2656693
29. Mudhasani R, Puri V, Hoover K, Czech MP, Imbalzano AN, Jones SN. Dicer is required for the formation of white but not brown adipose tissue. J Cell Physiol 2011; 226:1399-406; PMID:20945399; http://dx.doi.org/10.1002/jcp.22475
30. Wang Q, Li YC, Wang J, Kong J, Qi Y, Quigg RJ, Li X. miR-17-92 cluster accelerates adipocyte differentiation by negatively regulating tumor-suppressor Rb2/p130. Proc Natl Acad Sci U S A 2008; 105:2889-94; PMID:18287052; http://dx.doi.org/10.1073/pnas.0800178105
31. Karbiener M, Fischer C, Nowitsch S, Opriessnig P, Papak C, Ailhaud G, Dani C, Amri EZ, Scheideler M. microRNA miR-27b impairs human adipocyte differentiation and targets PPARgamma. Biochem Biophys Res Commun 2009; 390:247-51; PMID:19800867; http://dx.doi.org/10.1016/j.bbrc.2009.09.098
32. Kim SY, Kim AY, Lee HW, Son YH, Lee GY, Lee JW, Lee YS, Kim JB. miR-27a is a negative regulator of adipocyte differentiation via suppressing PPARgamma expression. Biochem Biophys Res Commun 2010; 392:323-8; PMID:20060380; http://dx.doi.org/10.1016/j.bbrc.2010.01.012
33. Lin Q, Gao Z, Alarcon RM, Ye J, Yun Z. A role of miR-27 in the regulation of adipogenesis. FEBS J 2009; 276:2348-58; PMID:19348006; http://dx.doi.org/10.1111/j.1742-4658.2009.06967.x
34. Schoolmeesters A, Eklund T, Leake D, Vermeulen A, Smith Q, Force Aldred S, Fedorov Y. Functional profiling reveals critical role for miRNA in differentiation of human mesenchymal stem cells. PLoS One 2009; 4:e5605; PMID:19440384; http://dx.doi.org/10.1371/journal.pone.0005605
35. Hassan MQ, Gordon JAR, Beloti MM, Croce CM, van Wijnen AJ, Stein JL, Stein GS, Lian JB. A network connecting Runx2, SATB2, and the miR-23a~27a~24-2 cluster regulates the osteoblast differentiation program. Proc Natl Acad Sci U S A 2010; 107:19879-84; PMID:20980664; http://dx.doi.org/10.1073/pnas.1007698107
36. Li Z, Hassan MQ, Jafferji M, Aqeilan RI, Garzon R, Croce CM, van Wijnen AJ, Stein JL, Stein GS, Lian JB. Biological functions of miR-29b contribute to positive regulation of osteoblast differentiation. J Biol Chem 2009; 284:15676-84; PMID:19342382; http://dx.doi.org/10.1074/jbc.M809787200
37. Kajimoto K, Naraba H, Iwai N. MicroRNA and 3T3-L1 pre-adipocyte differentiation. RNA 2006; 12:1626-32; PMID:16870994; http://dx.doi.org/10.1261/rna.7228806
38. He A, Zhu L, Gupta N, Chang Y, Fang F. Overexpression of micro ribonucleic acid 29, highly up-regulated in diabetic rats, leads to insulin resistance in 3T3-L1 adipocytes. Mol Endocrinol 2007; 21:2785-94; PMID:17652184; http://dx.doi.org/10.1210/me.2007-0167
39. Ortega FJ, Moreno-Navarrete JM, Pardo G, Sabater M, Hummel M, Ferrer A, Rodriguez-Hermosa JI, Ruiz B, Ricart W, Peral B, et al. MiRNA expression profile of human subcutaneous adipose and during adipocyte differentiation. PLoS One 2010; 5:e9022; PMID:20126310; http://dx.doi.org/10.1371/journal.pone.0009022
40. Galhardo M, Sinkkonen L, Berninger P, Lin J, Sauter T, Heinäniemi M. Integrated analysis of transcript-level regulation of metabolism reveals disease-relevant nodes of the human metabolic network. Nucleic Acids Res 2013; (Forthcoming); PMID:24198249; http://dx.doi.org/10.1093/nar/gkt989
41. Herrera BM, Lockstone HE, Taylor JM, Ria M, Barrett A, Collins S, Kaisaki P, Argoud K, Fernandez C, Travers ME, et al. Global microRNA expression profiles in insulin target tissues in a spontaneous rat model of type 2 diabetes. Diabetologia 2010; 53:1099-109; PMID:20198361; http://dx.doi.org/10.1007/s00125-010-1667-2
42. Mikkelsen TS, Xu Z, Zhang X, Wang L, Gimble JM, Lander ES, Rosen ED. Comparative epigenomic analysis of murine and human adipogenesis. Cell 2010; 143:156-69; PMID:20887899; http://dx.doi.org/10.1016/j.cell.2010.09.006
43. Hamm JK, Park BH, Farmer SR. A role for C/EBPbeta in regulating peroxisome proliferator-activated receptor gamma activity during adipogenesis in 3T3-L1 preadipocytes. J Biol Chem 2001; 276:18464-71; PMID:11279134; http://dx.doi.org/10.1074/jbc.M100797200
44. Waite KJ, Floyd ZE, Arbour-Reily P, Stephens JM. Interferon-gamma-induced regulation of peroxisome proliferator-activated receptor gamma and STATs in adipocytes. J Biol Chem 2001; 276:7062-8; PMID:11106650; http://dx.doi.org/10.1074/jbc.M007894200
45. MacDougald OA, Cornelius P, Lin FT, Chen SS, Lane MD. Glucocorticoids reciprocally regulate expression of the CCAAT/enhancer-binding protein alpha and delta genes in 3T3-L1 adipocytes and white adipose tissue. J Biol Chem 1994; 269:19041-7; PMID:8034662
46. Tontonoz P, Hu E, Spiegelman BM. Stimulation of adipogenesis in fibroblasts by PPAR γ 2, a lipid-activated transcription factor. Cell 1994; 79:1147-56; PMID:8001151; http://dx.doi.org/10.1016/0092-8674(94)90006-X
47. Olivecrona G, Olivecrona T. Triglyceride lipases and atherosclerosis. Curr Opin Lipidol 2010; 21:409-15; PMID:20683326; http://dx.doi.org/10.1097/MOL.0b013e32833ded83
48. Staels B, Schoonjans K, Fruchart JC, Auwerx J. The effects of fibrates and thiazolidinediones on plasma triglyceride metabolism are mediated by distinct peroxisome proliferator activated receptors (PPARs). Biochimie 1997; 79:95-9; PMID:9209702; http://dx.doi.org/10.1016/S0300-9084(97)81497-6
49. Takahashi M, Yagyu H, Tazoe F, Nagashima S, Ohshiro T, Okada K, Osuga J, Goldberg IJ, Ishibashi S. Macrophage lipoprotein lipase modulates the development of atherosclerosis but not adiposity. J Lipid Res 2013; 54:1124-34; PMID:23378601; http://dx.doi.org/10.1194/jlr.M035568
50. Mamputu JC, Levesque L, Renier G. Proliferative effect of lipoprotein lipase on human vascular smooth muscle cells. Arterioscler Thromb Vasc Biol 2000; 20:2212-9; PMID:11031206; http://dx.doi.org/10.1161/01.ATV.20.10.2212
51. Ranganathan G, Li C, Kern PA. The translational regulation of lipoprotein lipase in diabetic rats involves the 3′-untranslated region of the lipoprotein lipase mRNA. J Biol Chem 2000; 275:40986-91; PMID:11024042; http://dx.doi.org/10.1074/jbc.M008775200
52. Ahn J, Lee H, Chung CH, Ha T. High fat diet induced downregulation of microRNA-467b increased lipoprotein lipase in hepatic steatosis. Biochem Biophys Res Commun 2011; 414:664-9; PMID:21986524; http://dx.doi.org/10.1016/j.bbrc.2011.09.120
53. Chen T, Li Z, Tu J, Zhu W, Ge J, Zheng X, Yang L, Pan X, Yan H, Zhu J. MicroRNA-29a regulates pro-inflammatory cytokine secretion and scavenger receptor expression by targeting LPL in oxLDL-stimulated dendritic cells. FEBS Lett 2011; 585:657-63; PMID:21276447; http://dx.doi.org/10.1016/j.febslet.2011.01.027
54. Mangan S, Alon U. Structure and function of the feed-forward loop network motif. Proc Natl Acad Sci U S A 2003; 100:11980-5; PMID:14530388; http://dx.doi.org/10.1073/pnas.2133841100

55. Ebert MS, Sharp PA. Roles for microRNAs in conferring robustness to biological processes. Cell 2012; 149:515-24; PMID:22541426; http://dx.doi.org/10.1016/j.cell.2012.04.005
56. Vickers KC, Shoucri BM, Levin MG, Wu H, Pearson DS, Osei-Hwedieh D, Collins FS, Remaley AT, Sethupathy P. MicroRNA-27b is a regulatory hub in lipid metabolism and is altered in dyslipidemia. Hepatology 2013; 57:533-42; PMID:22777896; http://dx.doi.org/10.1002/hep.25846
57. Lewis BP, Burge CB, Bartel DP. Conserved seed pairing, often flanked by adenosines, indicates that thousands of human genes are microRNA targets. Cell 2005; 120:15-20; PMID:15652477; http://dx.doi.org/10.1016/j.cell.2004.12.035
58. John E, Wienecke-Baldacchino A, Liivrand M, Heinäniemi M, Carlberg C, Sinkkonen L. Dataset integration identifies transcriptional regulation of microRNA genes by PPARγ in differentiating mouse 3T3-L1 adipocytes. Nucleic Acids Res 2012; 40:4446-60; PMID:22319216; http://dx.doi.org/10.1093/nar/gks025
59. Petrovic N, Walden TB, Shabalina IG, Timmons JA, Cannon B, Nedergaard J. Chronic peroxisome proliferator-activated receptor gamma (PPARgamma) activation of epididymally derived white adipocyte cultures reveals a population of thermogenically competent, UCP1-containing adipocytes molecularly distinct from classic brown adipocytes. J Biol Chem 2010; 285:7153-64; PMID:20028987; http://dx.doi.org/10.1074/jbc.M109.053942
60. Schmidt H, Jirstrand M. Systems Biology Toolbox for MATLAB: a computational platform for research in systems biology. Bioinformatics 2006; 22:514-5; PMID:16317076; http://dx.doi.org/10.1093/bioinformatics/bti799
61. Vaz AIF, Vicente LN. A particle swarm pattern search method for bound constrained global optimization. J Glob Optim 2007; 39:197-219; http://dx.doi.org/10.1007/s10898-007-9133-5
62. Winkler J. Numerical recipes in C: The art of scientific computing. In: W.H. Press, S.A. Teukolsky, W.T. Vetterling, B.P. Flannery, ed(s). Second edition. Cambridge University Press. Endeavour. 1993;17(4):201.
63. Le Novère N, Hucka M, Mi H, Moodie S, Schreiber F, Sorokin A, Demir E, Wegner K, Aladjem MI, Wimalaratne SM, et al. The Systems Biology Graphical Notation. Nat Biotechnol 2009; 27:735-41; PMID:19668183; http://dx.doi.org/10.1038/nbt.1558